Plasmonic noise in nanometric semiconductor layers

2009 J. Stat. Mech. 2009 P02030

(http://iopscience.iop.org/1742-5468/2009/02/P02030)

Journal of Statistical Mechanics: Theory and Experiment
An IOP and SISSA journal

Plasmonic noise in nanometric semiconductor layers

J-F Millithaler[1], L Reggiani[1], J Pousset[2], L Varani[2], C Palermo[2], J Mateos[3], T González[3], S Perez[3] and D Pardo[3]

[1] Dipartimento di Ingegneria dell'Innovazione and CNISM, Università del Salento, Via Arnesano s/n, 73100 Lecce, Italy
[2] Institut d'Électronique du Sud, UMR CNRS 5214, Université Montpellier II, place Bataillon, 34095 Montpellier Cedex 5, France
[3] Departamento de Fisicà Aplicada, Universidad de Salamanca, Plaza Merced s/n 37008 Salamanca, Spain
E-mail: jf.millithaler@unile.it, lino.reggiani@unile.it, pousset@cem2.univ-montp2.fr, luca.varani@ies.univ-montp2.fr, christophe.palermo@ies.univ-montp2.fr, javierm@usal.es, tomasg@usal.es, susana@usal.es and dpardo@usal.es

Received 14 November 2008
Accepted 8 December 2008
Published 11 February 2009

Online at stacks.iop.org/JSTAT/2009/P02030
doi:10.1088/1742-5468/2009/02/P02030

Abstract. By means of numerical simulations we investigate voltage and current fluctuation spectra of an n-type $In_{0.53}Ga_{0.47}As$ layer of thickness W and submicron length L at $T = 300$ K. In agreement with theoretical expectations, for a plasma time longer than the dielectric relaxation time, the spectral density of the voltage fluctuations is found to peak at the plasma frequency before cut-off. For $W = 100$ nm and carrier concentrations of 10^{16}–10^{18} cm^{-3} the results of simulations reproduce the standard 3D expression for the plasma frequency. For $W \leq 10$ nm the results exhibit a plasma frequency (plasmonic noise) that depends on L, thus implying that the oscillation mode is dispersive. The corresponding frequency values are in good qualitative agreement with the 2D expression for the plasma frequency obtained for a collisionless analytical model using the in-plane approximation for the electric field. A set of novel results not predicted by the analytical model are particularized and discussed.

Keywords: classical Monte Carlo simulations, current fluctuations

1742-5468/09/P02030+12$30.00

Contents

1. Introduction

Generation and detection of electromagnetic radiation in the terahertz (THz) domain are seeing fast development because of the potential applications in different branches of advanced technologies, such as broadband communications, high resolution spectroscopy, medical and biological imaging, security, etc [1, 2]. Experimentally, both THz emission [3]–[5] and detection [6]–[8] were achieved with nanometric devices, and a recent overview on theoretical and experimental findings can be found in [9]. As a consequence, the realization of solid-state devices operating in the THz domain at room temperature and with compact, powerful, and tunable characteristics is mandatory.

One of the most promising strategies to this end lies in the plasmonic approach, which exploits the plasma frequency associated with long range Coulomb interaction of charge carriers. Recently, the concept of resonant detectors in which a plasma resonant cavity is integrated with a Schottky junction was proposed and substantiated [10, 11].

For bulk semiconductors, the plasma frequency is given by the simple expression [12]

$$f_{\mathrm{p}}^{\mathrm{3D}} = \frac{1}{2\pi}\sqrt{\frac{e^2 n_0^{\mathrm{3D}}}{m_0 m \varepsilon_0 \varepsilon_{\mathrm{mat}}}} \tag{1}$$

with n_0^{3D} the three-dimensional (3D) average carrier concentration, m_0 and m the free and effective electron masses, respectively, and ε_0, $\varepsilon_{\mathrm{mat}}$ the vacuum permittivity and the relative dielectric constant of the bulk material, respectively. For carrier concentrations of about 10^{17} cm^{-3} the plasma frequency is in the THz range for most materials.

On the other hand, for semiconductor layers embedded in an external dielectric and of width W sufficiently small (nanometer range) to justify the in-plane approximation for the solution of the Poisson equation, it was found that the plasma frequency and its higher harmonics are given by [13]

$$f_{\mathrm{p}}^{\mathrm{2D}} = \frac{1}{2\pi}\sqrt{\frac{e^2 n_0^{\mathrm{2D}} k}{2 m_0 m \varepsilon_0 \varepsilon_{\mathrm{diel}}}(2l-1)} \tag{2}$$

where n_0^{2D} is the average two-dimensional (2D) carrier concentration, $\varepsilon_{\mathrm{diel}}$ the relative dielectric constant of the external dielectric, k the wavevector, $l = 1, 2, 3, \ldots$ with the

fundamental mode ($l = 1$) given by $k = \pi/2L$ with L the length of the layer (implying that $\lambda = 2\pi/k$ with λ the plasma wavelength) for boundary conditions corresponding to zero ac potential at the source and zero current at the drain contact, respectively. We notice that the 2D plasma frequency is dispersive, i.e. $f_{\rm p}^{\rm 2D} = f_{\rm p}^{\rm 2D}(k)$, and depends on the relative dielectric constant of the external dielectric.

In this paper we will report a theoretical investigation on the plasma frequency associated with the long range Coulomb interaction among free carriers, here called plasmonic noise because it is detectable in voltage noise spectra already under thermal equilibrium conditions. As the physical system we consider an n-type $In_{0.53}Ga_{0.47}As$ layer of nanometric thickness W in the range 1–100 nm and variable length L in the range 0.001–1 μm embedded in a dielectric medium (the vacuum) operating at room temperature. We further assume that $n_0^{\rm 2D} = n_0^{\rm 3D} W$.

Unlike a previous investigation on the subject [14], ours analyzes both voltage and current fluctuations over the steady state, thus providing a complete view of the conditions under which plasmonic resonances can be evidenced or reduced in the system. In particular, we will focus on short channel lengths to study the transition between diffusive and ballistic transport regimes and, in addition to thermal equilibrium conditions, we consider also high field transport where Gunn oscillations can compete with plasma oscillations. In this way, we are in the position to compare plasmonic features obtained by analytical approaches tailored using simple transport models based on a parabolic effective mass, a relaxation time assumption, etc, with those pertaining to a more detailed physical model where transport is treated in a self-consistent Monte Carlo approach which couples instantaneously the microscopic dynamics with the solution of the Poisson equation. Because of the above, what we are presenting should answer several questions recently raised by several theoretical and experimental groups at the Unsolved Problems of Noise conference [15].

The content of the paper is organized as follows. Section 2 presents the theoretical approach. Results are discussed in section 3. Major conclusions are drawn in section 4.

2. Theory

Theoretical calculations are carried out by using an ensemble Monte Carlo simulator self-consistently coupled with a two-dimensional (2D) Poisson solver and in the presence of an external applied voltage as already detailed in [4, 16].

The structure of the device under test (DUT), which is depicted in figure 1, represents a simplified version of an ungated transistor channel. The bar is surrounded by a perfect dielectric (here taken as the vacuum), 10 μm wide in the upper and lower regions of the bar, where the 2D Poisson equation in the xz-plane is solved to account for the fringing of the external electric field [17]. The third dimension is used to relate the number of simulated carriers with the 3D carrier concentration.

The time and space discretizations take typical values of 0.2–1 fs for the time step, 0.1–5 nm for the spatial scale of the bar and 500 nm for the spatial scale of the dielectric. Typically there are about 80 carriers inside a mesh of the bar, which are found to provide a reliable solution of the Poisson equation. The extracted potential $V(t)$ is usually taken at the center of the bar while the fluctuations of current $I(t)$ are taken at the second contact of the DUT (see figure 1). The contacts are realized by an infinite reservoir of

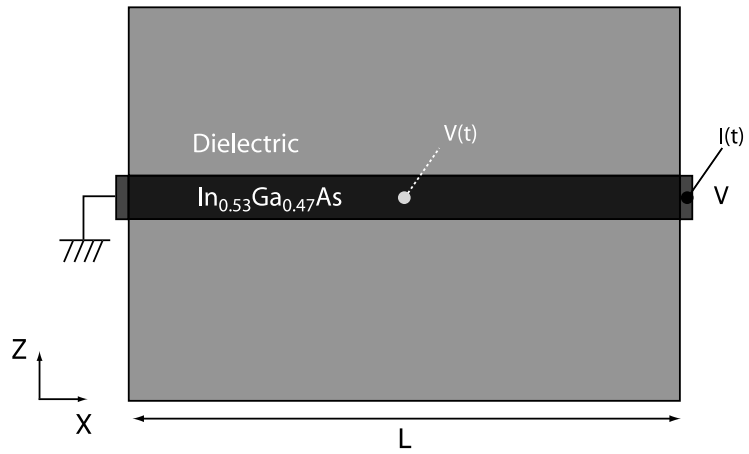

Figure 1. Schematic of the DUT (not in scale) studied within the Monte Carlo simulation. The free charge is present only in the bar made of n-type $In_{0.53}Ga_{0.47}As$ of length L along the x direction and thickness W along the z direction. The terminals on the right-and left-hand sides are kept at given constant voltages and are connected to ideal thermal reservoirs of electrons which are injected at a constant rate into the bar. Carriers exiting the boundaries are lost.

thermalized electrons at electrochemical potentials differing by eU with U the applied voltage [18].

The presence of two contacts (2c), both taken at a fixed potential, modifies the boundary conditions with respect to the case of a single Ohmic contact (1c) at the source and a floating one at the drain considered in a previous work [14, 19]. As a consequence, for the same layer length L, the value of the 2D plasma frequency is expected to shift to a value lower by a factor of $1/\sqrt{2}$ (geometrical factor) with respect to the case of only one contact at a fixed potential (1c). This is in agreement with the relation $f_{\rm p}(1{\rm c}, L) = f_{\rm p}(2{\rm c}, 2L)$, which has been confirmed by MC simulations. We stress that we could not apply the boundary conditions of the analytical approach [13] to our simulator, because of the presence of an instantaneous current (displacement or conductive) at the drain. Accordingly, the agreement between the predictions of equation (2) and the results of numerical simulations can differ for a factor of the order of 2.

By evaluating the fluctuations of the voltage (current) around the steady value, the spectral density of these quantities is obtained from the corresponding correlation function. The characteristic peaks and the cut-off exhibited by the spectra are analyzed as detailed in [19]. We remark that, at low applied voltages, the DUT exhibits an Ohmic behavior in the current–voltage characteristics. At high applied voltages, the DUT exhibits a saturation behavior of the current.

In section 3 we investigate the spectral densities of both voltage and current fluctuations by focusing on their behavior in the high frequency range 10^{-2}–10^{2} THz. At these frequencies the interplay among the characteristic frequencies of the systems (i.e. collision rate, plasma, dielectric relaxation rate, Gunn domains) and their dependence upon the relevant parameters of the system and the applied bias is analyzed and compared with the predictions from existing analytical models.

J. Stat. Mech. (2009) P02030

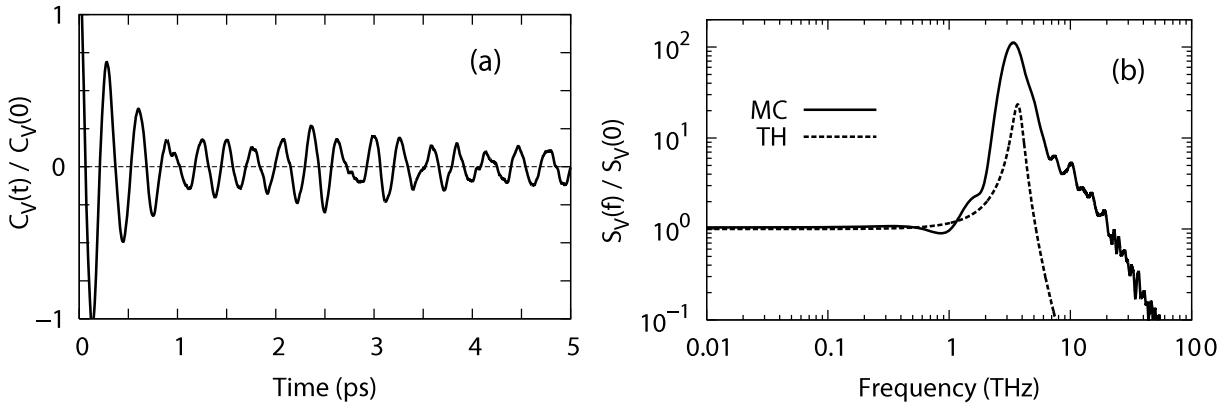

Figure 2. (a) Typical autocorrelation function of voltage fluctuations and (b) associated spectral density of the DUT for a thickness $W = 100$ nm with $n_0^{3D} = 10^{18}$ cm^{-3} and $L = 0.1$ μm at room temperature.

3. Results and discussion

To illustrate the results for the simulator used for the comparison with analytical predictions, figure 2 reports a typical correlation function and the associated spectrum of voltage fluctuations, $S_V(f)$, normalized to its zero-frequency value for the DUT for the case of $L = 0.1$ μm, $W = 100$ nm, $n_0^{3D} = 10^{17}$ cm^{-3} in the absence of an applied voltage. The results of the simulation (dotted curve) compare favorably with those obtained from the 3D impedance equivalent circuit (continuous curve) [20]:

$$\frac{S_V(f)}{S_V(0)} = \frac{1}{[1-(2\pi f\tau_p)^2]^2 + (2\pi f\tau_d)^2} \tag{3}$$

with f the frequency, $\tau_p = 4.28\times10^{-14}$ s, and $\tau_d = 1.81\times10^{-14}$ s the plasma and dielectric relaxation times corresponding to the simulated bulk material. Here, the plasma peak is well evidenced by the good qualitative fit between numerical and theoretical results which validates the numerical approach. We notice that the relevance of the agreement mostly refers to the position of the plasma peak, since the amplitude of the peak depends on the time window used for the Fourier transform of the correlation function. Furthermore, simulations evidence a cut-off decay as f^{-2}, which is reminiscent of the presence of scattering mechanisms, instead of the sharper f^{-4} predicted by the equivalent circuit model.

Figure 3 reports the correlation function and associated spectrum of current fluctuations, $S_I(f)$, normalized to its zero-frequency value for the same case as in figure 2. The results of the simulation (dotted curve) are compared with those obtained from the 3D impedance equivalent circuit (continuous curve) [20]:

$$\frac{S_I(f)}{S_I(0)} = \frac{1}{[1+(2\pi f\tau_c)^2]} \tag{4}$$

with $\tau_c = 1.07\times10^{-13}$ s the momentum relaxation time corresponding to the simulated bulk material. Here, as expected, the plasma peak is not evidenced and we find a good

J. Stat. Mech. (2009) P02030

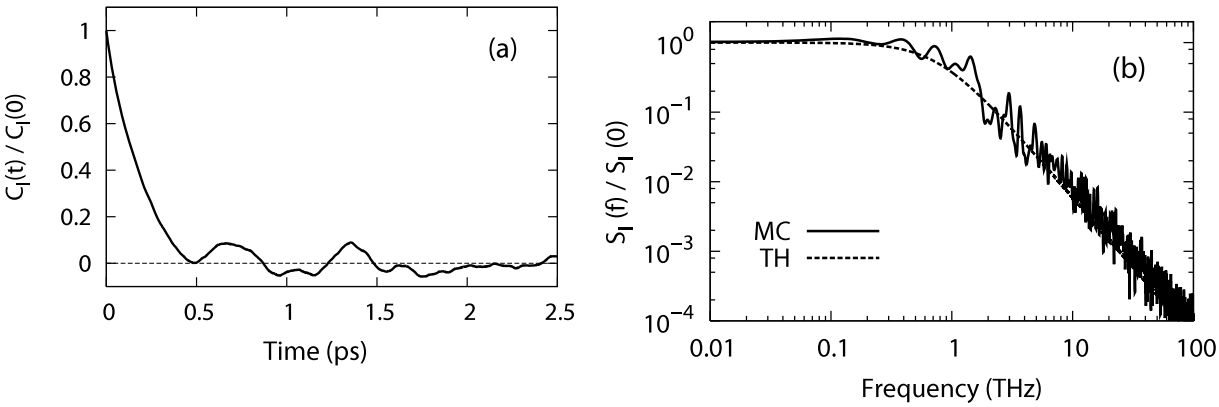

Figure 3. (a) Typical autocorrelation function of current fluctuations and (b) associated spectral density of the DUT with the same conditions as for figure 2.

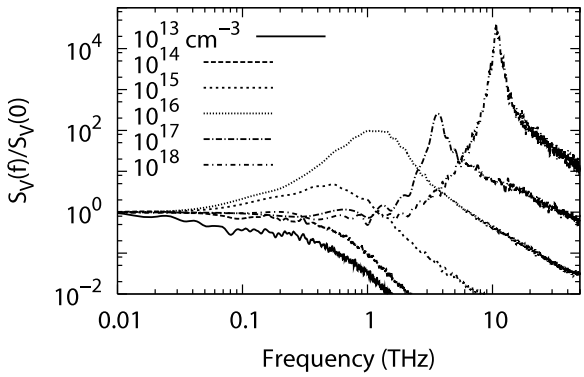

Figure 4. Spectral density of voltage fluctuations normalized to the static value of the DUT for different carrier concentrations with the same conditions as for figure 2.

quantitative fit between numerical and theoretical results, which further validates the numerical approach.

Figure 4 reports the set of voltage spectral densities at different carrier concentrations of the simulated bulk material. The 3D plasma peak is resolved down to $n^{3D} = 10^{15}$ cm^{-3} and the peak frequency is found to be in good agreement with the value predicted from equation (1). For $n^{3D} < 10^{15}$ cm^{-3} the plasma peak is no longer resolved because the plasma time becomes comparable to or shorter than the dielectric relaxation time.

Figure 5 presents the values of the plasma peak of the 2D case normalized to that of the 3D plasma peak as a function of the layer width. Here we have reported the normalized plasma frequencies obtained from simulations for lengths covering the range of values 0.1–1 μm and for 3D carrier concentrations in the range 10^{16}–10^{18} cm^{-3}, as bars. We have also reported the normalized theoretical values predicted from equation (1) (horizontal continuous line) and equation (2) with $l = 1$ and $k = \pi/L$ (shaded region). The agreement between numerical results (bars) and analytical (shaded region) expectations is within

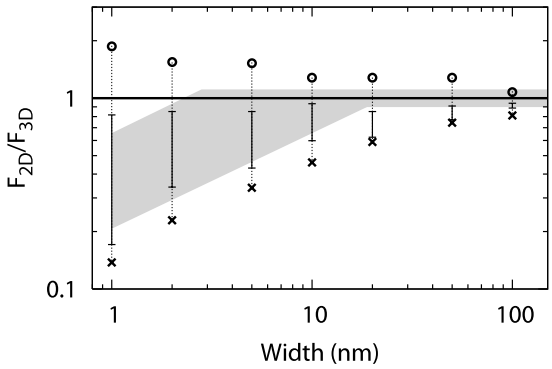

Figure 5. 2D plasma frequency normalized to the 3D value of the DUT as a function of the channel width for an electron density $n_0^{3D} = 10^{16}$–10^{18} cm^{-3}. The continuous line refers to the 3D form of equation (1), the shaded region refers to the 2D form of equation (2) covering the two cases of $L = 0.1$–1 μm, the dashed bars refer to Monte Carlo results covering the same two cases and include the numerical uncertainty estimated as within 20%.

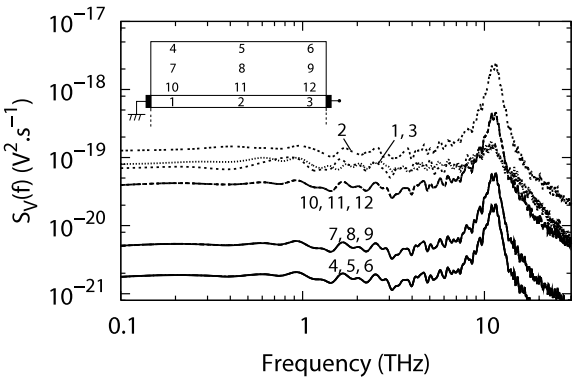

Figure 6. Spectral density of voltage fluctuations of the DUT detected at different points inside the conducting layer and inside the external dielectric as sketched in the inset.

numerical uncertainty, and thus considered to be satisfactory. We notice that the results evidence the constraint $f_p^{2D} \leq f_p^{3D}$ associated with the intrinsic characteristic of numerical simulations.

Figure 6 reports the voltage spectral densities sampled at different points of the structure under test. Spectra 1, 2 and 3 refer to regions close to, respectively, the left contact, the center, and the right contact of the conductive channel. Here, the plasma peak is found to be strongly suppressed in the contact regions since there the potential is fixed. The other curves are related to the dielectric region as shown in the inset. There, the spectra are found to keep the same shape as spectrum 2, with an amplitude which decreases significantly with the distance from the conducting channel. In other words, voltage fluctuations propagate from the conducting source into the insulating medium where their amplitudes are suppressed at increasing distances from the channel because of the evanescent modes of the electric field.

J. Stat. Mech. (2009) P02030

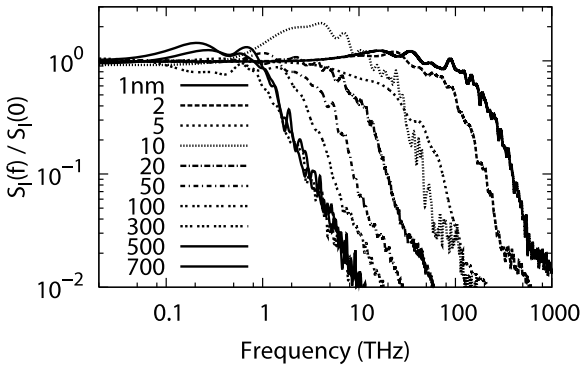

Figure 7. Spectral density of current fluctuations normalized to the static value of the DUT for different values of the layer length.

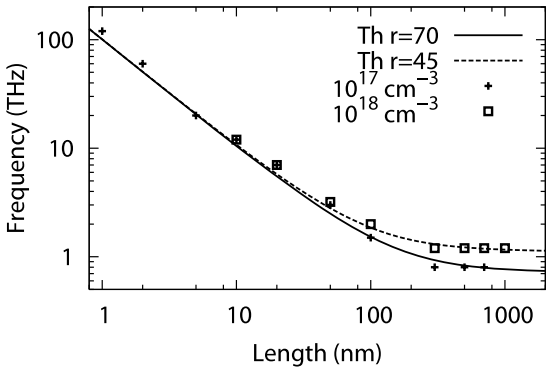

Figure 8. Cut-off frequency of the current fluctuation spectra of figure 7 showing the transition from the diffusive transport regime to the ballistic one.

The results concerning the spectral density of current fluctuations under thermal equilibrium conditions are summarized in figure 7, which reports the normalized spectral densities for the case of $W = 1$ nm, $n_0^{3D} = 10^{17}$ cm^{-3} and for different layer lengths. Results show that the cut-off region extends to high frequencies for lengths below about 100 nm, concomitant with the onset of the ballistic transport regime. The cut-off frequency associated with each length is reported in figure 8. Here, the transition from a ballistic to a diffusive transport regime is found to agree well with the analytical expression deduced from [21]:

$$f(L) = \frac{1}{2\pi}\frac{v_{\mathrm{th}}}{L}\frac{1}{\Gamma(r)} \tag{5}$$

where

$$\Gamma(r) = 2r\{1 - r[1 - \exp(-r^{-1})]\} \tag{6}$$

and with $r = \tau_{\mathrm{m}}/\tau_{\mathrm{T}} = 1.09\, l/L$, where τ_{m} is the collision time, $\tau_{\mathrm{T}} = L/v_0$ is the ballistic transit time, with $v_0 = (8k_{\mathrm{B}}T/\pi m m_0)^{1/2}$ the oriented thermal velocity, and $l = v_{\mathrm{th}}\tau_{\mathrm{m}}$ is the carrier mean free path, with $v_{\mathrm{th}} = (2k_{\mathrm{B}}T/3mm_0)^{1/2}$ the thermal carrier velocity. The values of $r = 45$ and 70 provide the best fitting and correspond well to the different collision times for the two levels of doping considered.

J. Stat. Mech. (2009) P02030

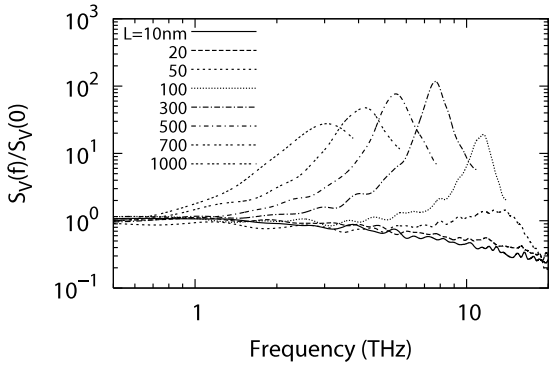

Figure 9. Spectral density of voltage fluctuations normalized to the static value of the DUT for different values of the layer length for a thickness $W = 1$ nm and for a free electron density of $n_0^{3D} = 10^{18}$ cm^{-3}.

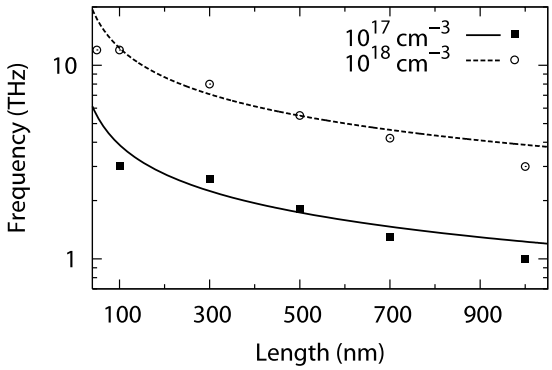

Figure 10. Plasma frequencies of the DUT for electron densities $n_0^{3D} = 10^{17}$ and 10^{18} cm^{-3} in the diffusive transport regime. Symbols refer to numerical simulations, curves to the analytical expression of equation (2) with $k = \pi/L$.

The results concerning the spectral density of voltage fluctuations under thermal equilibrium conditions are summarized in figure 9, which reports the normalized spectral densities of voltage fluctuation for the case of $W = 1$ nm, $n_0^{3D} = 10^{18}$ cm^{-3} at different lengths. Results show the onset of a peak in the spectrum for lengths above about 50 nm, and thus at the start of the diffusive transport regime. By contrast, for lengths shorter than 50 nm all spectra are flat and exhibit a beginning of a cut-off at about 5 THz, which is practically independent of the layer width. Remarkably, the shorter the layer length, the less pronounced the cut-off region.

Figure 10 reports the plasma frequencies as a function of the channel length in the diffusive transport regime for electron densities $n_0^{3D} = 10^{17}$ and 10^{18} cm^{-3}. The comparison with the fundamental frequency of the analytical model with $k = \pi/L$ (see the continuous curves) is found to be satisfactory.

Figure 11 reports the normalized spectral densities of voltage fluctuation for the case of $W = 1$ nm, $n_0^{3D} = 10^{18}$ cm^{-3} and $L = 0.3$ μm in the presence (WS) and in the absence (NS) of scattering. Analogous results have been obtained for the range of lengths

J. Stat. Mech. (2009) P02030

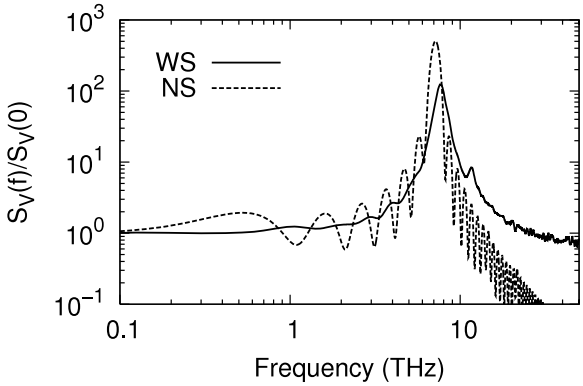

Figure 11. Spectral density of voltage fluctuations normalized to the static value of the DUT for a layer length of 300 nm, for a thickness $W = 1$ nm and for a free electron density of $n_0^{3D} = 10^{18}$ cm^{-3} obtained from simulations in the presence (WS) and absence (NS) of collisions.

0.05–1 μm. Apart from a wavy shape of the NS spectrum, we find that the plasma peak remains practically at the same frequency, thus confirming for these channel lengths its independence from the presence or absence of collisions.

Figure 12 compares the noise spectra of voltage fluctuations with those of current fluctuations at thermal equilibrium (figures 12(a) and (c)), and in the presence of an applied voltage (1 V) sufficiently high for the onset of Gunn instabilities [22] (figures 12(b) and (d)). Simulations are performed for the case of $W = 1$ nm, $n_0^{3D} = 10^{18}$ cm^{-3} and a layer length $L = 1$ μm. The results show that the presence of the Gunn instabilities suppresses the plasma peak of the voltage spectral density totally and is responsible for a sharp peak in both the voltage and current spectra at the Gunn domain transit time frequency of about 0.1 THz. We remark that the voltage spectrum at equilibrium evidences a second peak at the 3D plasma frequency, while the current spectrum at 1 V exhibits higher harmonics, up to four over the fundamental of the Gunn transit frequency.

4. Conclusions

We have carried out a microscopic investigation of plasmonic noise in nanochannels of $In_{0.53}Ga_{0.47}As$ embedded in an external dielectric. The subject has recently emerged as a hot one because of the practical interest in the development of electronic devices able to generate and/or detect microwaves in the terahertz domain. The results obtained using a realistic microscopic model based on a self-consistent Monte Carlo approach evidence a complicated scenario, only partly in agreement with what was predicted from a 2D analytical approach [13]. Major conclusions can be summarized as follows.

(i) Dispersion of the plasma frequency is present only above a threshold value of the length of the layer (typically 40 and 100 nm for carrier concentrations of 10^{18} and 10^{17}, respectively) and below a given value of the layer width (typically 10 nm).

J. Stat. Mech. (2009) P02030

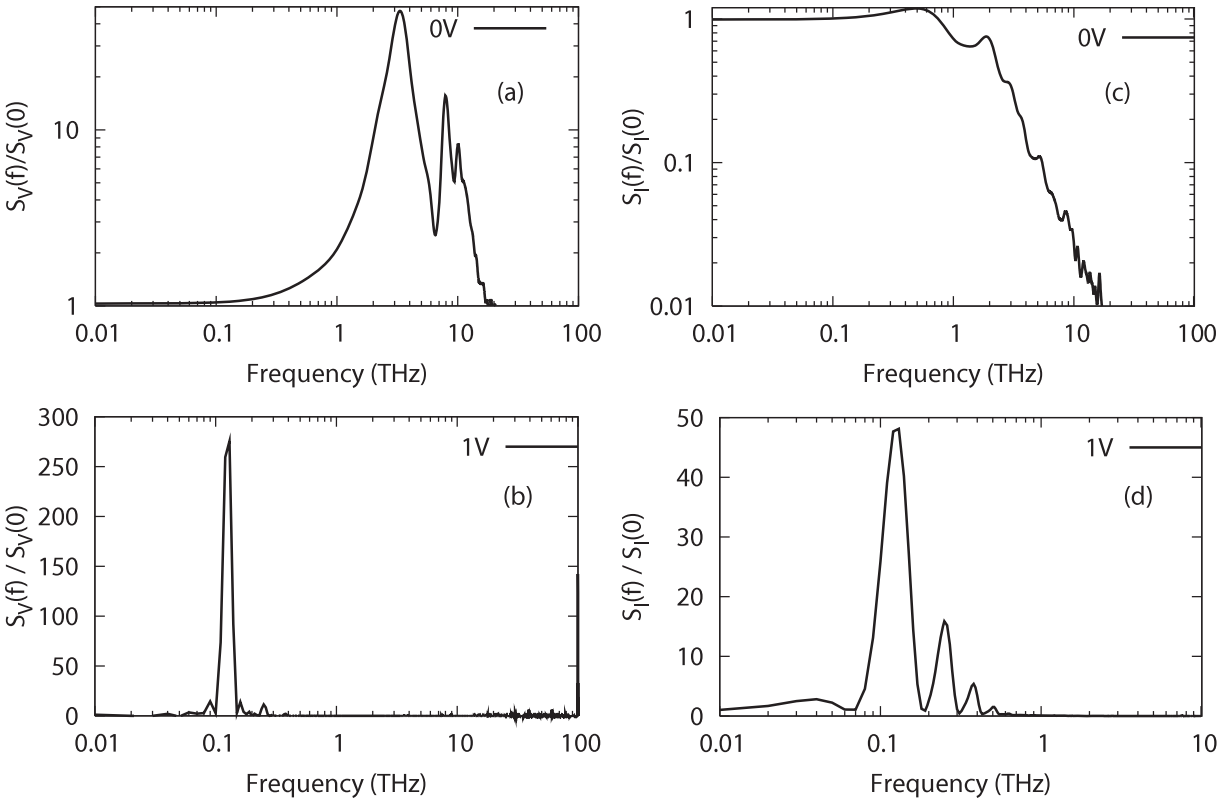

Figure 12. Voltage and current spectral densities of the DUT under thermal equilibrium conditions, (a) and (c), respectively, and in the presence of a bias $V = 1$ V, (b) and (d), respectively.

(ii) The presence of scattering does not qualitatively modify the main results concerning the plasma peak; indeed simulations provide the same results on switching off scattering.

(iii) The onset of a ballistic region starting from layer lengths below about 100 nm leads to the suppression of the plasma peak. Here only a cut-off region of the spectra is found.

(iv) The current spectral density does not evidence the plasma peak, as expected, but at high voltages it evidences peaks at the Gunn transit frequency in analogy with the case of the voltage spectral density.

Problems that remain open for further investigations are:

(i) For the shortest lengths the existence of a ballistic dielectric relaxation cut-off is not confirmed.

(ii) The formulation of an equivalent circuit able to describe the 2D case is still lacking.

(iii) The harmonics over the fundamental 2D plasmon frequency predicted by equation (2) have not been evidenced in numerical simulations.

(iv) A direct comparison of theory with experiments remains mostly an open challenge, where the boundary conditions are expected to play a major role [23].

J. Stat. Mech. (2009) P02030

Acknowledgments

The work was supported by CNRS—GDR and GDR-E projects 'Semiconductor sources and detectors of THz frequencies', the Region Languedoc–Roussillon project 'Platforme Technologique THz', the Dirección General de Investigación (MEC, Spain), the FEDER through the project TEC2007-61259MIC and the Action integrada HF 2007-0014, the Italy–France bilateral project Galileo 2007–2008, the Spain–France bilateral project Picasso 2007–2008.

References

[1] Mittleman D, Gupta M, Neelamani R, Baraniuk J, Rudd R and Koch M, 1999 *Appl. Phys.* B **68** 1085
[2] Wollard D L, Brown E R, Pepper M and Kemp M, 2005 *Proc. IEEE* **93** 1722
[3] Knap W, Lusakowski J, Parenty T, Bollaert S, Cappy A and Shur M S, 2004 *Appl. Phys. Lett.* **84** 2331
[4] Lusakowski J, Knap W, Dyakonova N, Varani L, Mateos J, González T, Roelens Y, Bollaert S, Cappy A and Karpierz K, 2005 *J. Appl. Phys.* **97** 064307
[5] Dyakonova N, ElFatimy A, Lusakowski J, Knap W, Dyakonov M I, Poisson M-A, Morvan E, Bollaert S, Shchepetov A, Roelens Y, Gaquiere Ch, Theron D and Cappy A, 2006 *Appl. Phys. Lett.* **88** 141906
[6] Ryzhii V, Satou A, Khmyrova I, Chaplik A and Shur M S, 2004 *J. Appl. Phys.* **96** 7625
[7] ElFatimy A, Teppe F, Dyakonova N, Knap W, Seli-uta D, Valusis G, Shchepetov A, Roelens Y, Bollaert S, Cappy A and Rumyantsev S, 2006 *Appl. Phys. Lett.* **89** 131926
[8] Ryzhii V, Satou A, Otsuji T and Shur M S, 2008 *J. Appl. Phys.* **103** 014504
[9] Ryzhii V (ed), 2008 *J. Phys.: Condens. Matter* **20** (38) Special section on heterostructure terahertz devices
[10] Ryzhii V and Shur M S, 2006 *Japan. J. Appl. Phys.* Part 2 **45** L1118
[11] Satou A, Vagidov N and Ryzhii V, 2006 *IEICE Tech. Rep.* p 77 ED2006-197
[12] Kittel C, 1966 *Introduction to Solid State Physics* (New York: Wiley)
[13] Dyakonov M and Shur M S, 2005 *Appl. Phys. Lett.* **87** 111501
[14] Millithaler J-F, Reggiani L, Pousset J, Sabatini G, Varani L, Palermo C, Mateos J, González T, Perez S and Pardo D, 2008 *J. Phys.: Condens. Matter* **20** 384210
[15] Ciliberto S (ed), 2009 *Proc of UPoN08 Conf.*; *J. Stat. Mech.* January
[16] Mateos J, González T, Pardo D, Hoël V and Cappy A, 2000 *IEEE Trans. Electron. Devices* **47** 1950
[17] Shur M and Ryzhii V, 2003 *Int. J. High Speed Electron. Syst.* **13** 575
[18] Bulashenko O M, Mateos J, Pardo D, González T, Reggiani L and Rubi J M, 1998 *Phys. Rev.* B **57** 1366
[19] Millithaler J-F, Reggiani L, Pousset J, Varani L, Palermo C, Knap W, Mateos J, González T, Perez S and Pardo D, 2008 *Appl. Phys. Lett.* **92** 042113
[20] Varani L and Reggiani L, 1994 *Riv. Nuovo Cimento* **17** 1
[21] Butcher P, 1998 *Phys. Rev.* B **58** 9639
[22] Kroemer H, 1964 *Proc. IEEE* **52** 1736
[23] Dyakonov M I, 2008 arXiv:0802.3780v1 [cond-mat.mes-hall]

J. Stat. Mech. (2009) P02030